FABRICATION OF MSM UV PHOTODETECTOR BASED ON ZnO FILMS SYNTHESIZED BY RF MAGNETRON SPUTTERING

HALIM AHMAD[1], MAT JOHAR ABDULLAH[2] & AJIS LEPIT[3]

[1,3] Faculty of Applied Sciences, Universiti Teknologi MARA, Sabah Branch, Locked Bag 71, 88997, Kota Kinabalu, Sabah
e-mail: [1] halim667@sabah.uitm.edu.my, [3] ajis@sabah.uitm.edu.my

[2] School of Physics, Universiti Sains Malaysia, 11800 Pulau Pinang.
e-mail: matjohar@usm.my

ABSTRACT

C-axis oriented ZnO films were deposited on SiO_2/Si substrates through RF magnetron sputtering, MSM UV photodetector using Ag/ZnO/Ag configuration were fabricated from the as prepared film while the heat treated film was used to fabricate MSM Schottky barrier UV photodetector using Al/ZnO/Ag configuration. The crystalline and optical quality of the film had improved after the heat treatment. It was found that the Schottky barrier heights as prepared and heat treated using Ag/ZnO interface was around 0.74 and 0.76 eV respectively. The leakage current was reduced from 18.6 mA to 0.6 µA at 5V after post deposition annealing when compared with that of as deposited ZnO.The Ag/ZnO/Ag configuration showed a faster decay time of 212 s.

Keywords: Zinc Oxide; UV; Photodetector

ABSTRAK

Filem ZnO berorientasikan paksi-*c* telah dimendapkan keatas substrat SiO_2/Si dengan kaedah percikan Magnetron RF. Penderia cahaya UV dengan konfigurasi Ag/ZnO/Ag telah digunakan untuk sampel filem ZnO asal manakala sampel film ZnO yang dirawat haba pula menggunakan konfigurasi Al/ZnO/Ag untuk menghasilkan penderia cahaya UV halangan Schottky. Kualiti Kristal dan optikal filem ZnO telah meningkat selepas rawatan haba. Didapati bahawa ketinggian halangan schottky pada sampel asal dan yang dirawat haba adalah pada 0.74 dan 0.76 masing-masing. Arus bocor telah menurun dari 18.6 mA pada 0.6 µA (voltaj 5V) selepas rawatan haba. Konfigurasi Ag/ZnO/Ag telah menunjukkan masa pereputan lebih pantas dengan nilai 212 s.

Kata kunci: Zink Oksida; UV; Penderia Cahaya

1. Introduction

ZnO as a II-VI semiconductor compound has recently become an attractive material due to its potential application for optoelectronic devices such as light emitting device (LED) operating in the blue/ultraviolet (UV) region of the spectrum (Ozgur et al., 2005; Chunfeng et al., 2015; Vishnu et al. 2016; Sandeep et al 2017;) and lately UV photodetectors (Jaber et al., 2016; Farhat et al., 2016; Ke et al. 2016). ZnO has large direct band gap energy of 3.37 eV at room temperature, along with large exciton binding energy (60 meV). ZnO was seen as an alternative to GaN as it is more resistant to radiation and having 2.4 times larger exciton binding energy (Park et al., 1966). Recently, UV photodetectors are becoming significant in number of areas such as UV astronomy, radiation dosimetry, reagent detectors and missile warning systems (Monroy et al., 2001; Chai et al. 2009). Metal-semiconductor-metal (MSM) structures such as Schottky barrier diodes and simple photoconductive devices are regularly applied as photodetectors. Schottky barrier diodes have some advantages over photoconductive devices such as the simplicity of fabrication, compatibility with field effect transistors and their improved performance. The reports of ZnO UV photodetector mainly focus on MSM structures

which contain ohmic contacts that are photoconductive based (Cheng et al., 2008; Shewale et al., 2015; Forat et al. 2016) and Schottky barrier based photovoltage type (Liang et al., 2001; Ghusoon et al., 2014; Shaivalini and Park 2015). UV light detection with ZnO has created a lot of interest for selective photodetector applications (365 nm) (Cheng et al., 2006; Yadav et al., 2007). The increasing interest in the sensor field has led many researchers to investigate the possibility of widening the band gap of ZnO by alloying with Cd and Mg to extend over UV-A, UV-B and UV-C region (Makino et al., 2001 and Ohtomo et al., 1998). Many techniques has been used to deposit c-axis oriented ZnO films including molecular beam epitaxy (MBE) (Tatsumi et al., 2004; Yan et al., 2015), metal organic chemical vapor deposition (MOCVD) (Kim et al., 2003 Boukadhaba et al. 2015), atomic layer deposition (ALD) (Yamada et al., 1997; Liu et al. 2017) , sol-gel technique (Tang et al., 1994; Mariana et al 2017), spray pyrolisis (Purica et al., 2002; Lehraki et al. 2012), pulse laser deposition(PLD) (Wang et al., 2009; André et al. 2017), photo-enhanced chemical vapor deposition (P-E CVD) (Lee et al., 2001), and radio frequency (RF) sputtering (Zhang et al., 2007; Girija et al., 2016; Kim et al. 2017). Hence, RF sputtering is by far the most common technique used to deposit ZnO films. The advantages of RF sputtering compared with other deposition techniques are dense layer formation, high deposition rate, low growth temperature, low cost and so on. In this paper we investigate the photoresponse characteristics of a highly c-axis oriented ZnO films through MSM and Schottky barrier photodetectors.

2. Experimental Details

The ZnO films were deposited on SiO_2/Si (100) substrates through RF magnetron sputtering. The SiO_2 layer was prepared by growing a 1 µm thick SiO_2 layer on Si (100) substrates by thermal oxidation. A high purity (99.99%) ZnO target of 76.2 mm diameter was used for the sputtering. The vacuum chamber was first evacuated to 5×10^{-5} mbar before the introduction of Argon as the sputtering gas. Deposition was carried out at a working pressure of 2.3×10^{-2} mbar. The target was pre sputtered for 5 min to remove any contaminants. The sputtering power was maintained at 200 W during deposition. The thickness of the ZnO film was approximately 1.2 µm. After the deposition process, the samples were divided into two groups; one group for the as prepared sample and the other one for those undergone a heat treatment process of annealing at 800 °C for 1 hr in Ar ambient. Two types of MSM photodetectors were fabricated. The first one consists of two Ag parallel electrode contacts deposited by thermal evaporation on the as prepared ZnO film. The second type consists of the same parallel electrode pattern but with different metal (Al and Ag contact) which were thermally evaporated on the heat treated ZnO film. The interval between the contacts was about 0.69 mm. The total active area of the contacts and the whole device was 27.85 mm^2 and 100 mm^2 respectively. The Ag/ZnO/Ag and Al/ZnO/Ag photodetector is assigned as device A and device B respectively. The photodetector was placed in a box and at a distant of 1 cm from the light source. The photoconductivity of the photodetector was measured by the Keithley 237 via a LABVIEW programming in air at room temperature. The light source used for these measurements was the 365 nm UV Nichia LED and the optical power of the light source was 3 mW. The structural morphologies of the deposited films were investigated by X-Ray Diffractometry (XRD) using PANalytical Xpert Pro MRD PW3040 and the surface morphologies were investigated by Atomic Force Microscopy (AFM) and Field effect Scanning electron Microscopy (Leo Supra 50VP). The optical properties of the films were investigated by photoluminescence spectroscopy (PL) using Jobin Yvon HR 800 UV.

3. Results and Analysis

Figure 1 shows the vertical cross sectional SEM images of the UV photodetector ZnO film, from which the columnar growth of the ZnO film can be observed.

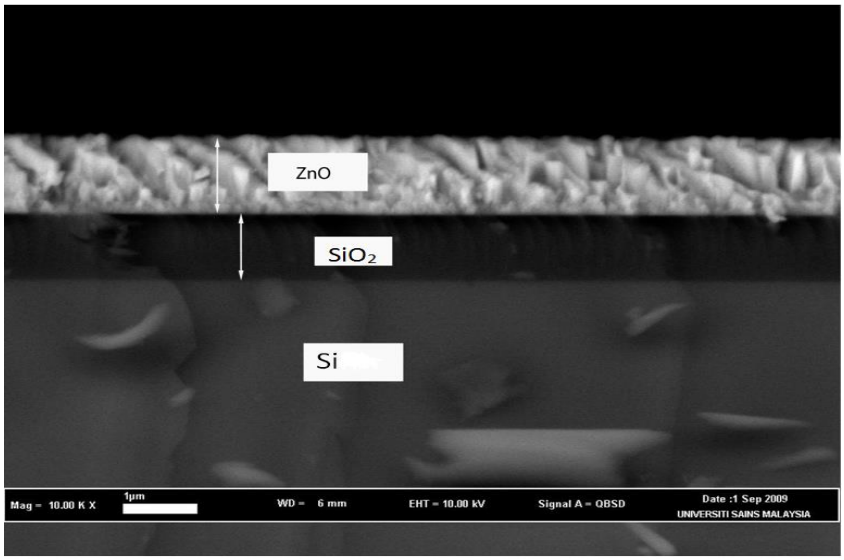

Figure 1: SEM image of the vertical cross-sectional view of as prepared ZnO film. [Magnification x10K].

Figure 2(a) to 2(d) show the topographic of three dimensional atomic force microscopy (AFM) images of the UV photodetector ZnO film. The images were produced utilizing non-contact mode with scan rate of 2.0 lines/s and scan area of 30X30 μm^2 and 5X5 μm^2. The AFM measurements were made on three different positions on both samples for statistical purpose. Figure 2(c) and 2(d) show that the heat treatment had induced an increased in the root mean square roughness which is 1.804 and 1.715 times larger in scale. The root mean square roughness of the as prepared sample is 39.66 nm for scanning area of 5X5 μm^2 and 30.99 nm for scanning area of 30X30 μm^2. For the heat treated samples the root mean square roughness is 71.55 nm and 53.15 nm for scanning area of 5X5 μm^2 and 30X30 μm^2 respectively. These results imply that the surface roughness increased after the as prepared ZnO thin film was heat treated at 800 °C. The sample exhibits larger gaps between the ZnO grains which provide space for oxygen to be absorbed through the surface and implanted into the bulk and then remained at the grain boundaries of the ZnO film. It is well known that the adsorption and photodesorption of oxygen significantly contributed to the photoresponsivity of ZnO semiconductors (Takahashi et al., 1994 and Li et al., 2005).

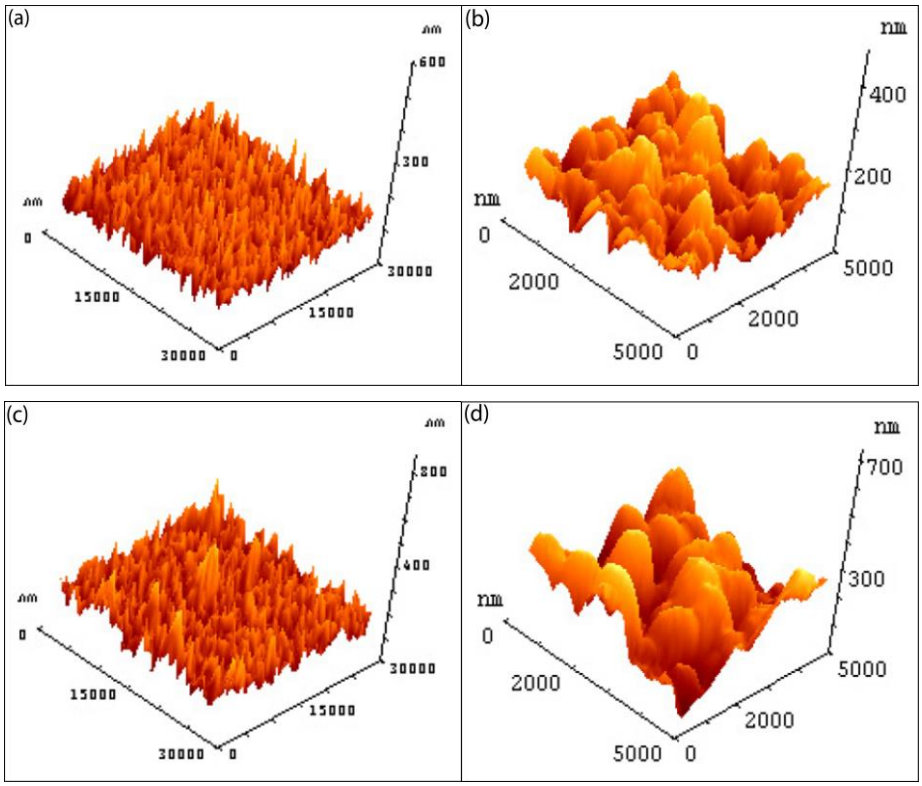

Figure 2: AFM image of the ZnO film: (a), (b)-before heat treatment, (c) and (d)-after heat treatment

Figure 3 shows the x-ray diffraction pattern for the prepared and heat treated ZnO film. It can be clearly seen that the crystal orientation is dominant of (002) phase with peaks at 34.3558 ° and 34.4560 ° for the as prepared and heat treated samples respectively. In addition, other diffractions peaks are observed for (101), (201) and (004) peaks, indicating the formation of a ZnO type hexagonal wurtzite crystal structure in accordance to ICSD Reference code: 01-079-0208 (Albertsson et al. 1989), which is typically obtained film structure deposited by RF magnetron sputtering (You et al. 1989). Two SiO_2 diffraction peaks were also observed at (110) and (105). The heat treated samples exhibited higher peaks intensity especially at the (002) peak. The ZnO (201) peak has been disappeared after heat treatment indicating good improvement in the crystalline quality of the ZnO film. The lattice spacing d_{002} obtained by the XRD data were 2.61034 Å and 2.60298 Å for the prepared and heat treated samples respectively, which yield the lattice constant c for both samples to be 5.22068 Å and 5.20596 Å as calculated using the equation $d_{002} = c/2$. The XRD results show that strong c-axis preferred orientation can be achieved through heat treatment of ZnO film.

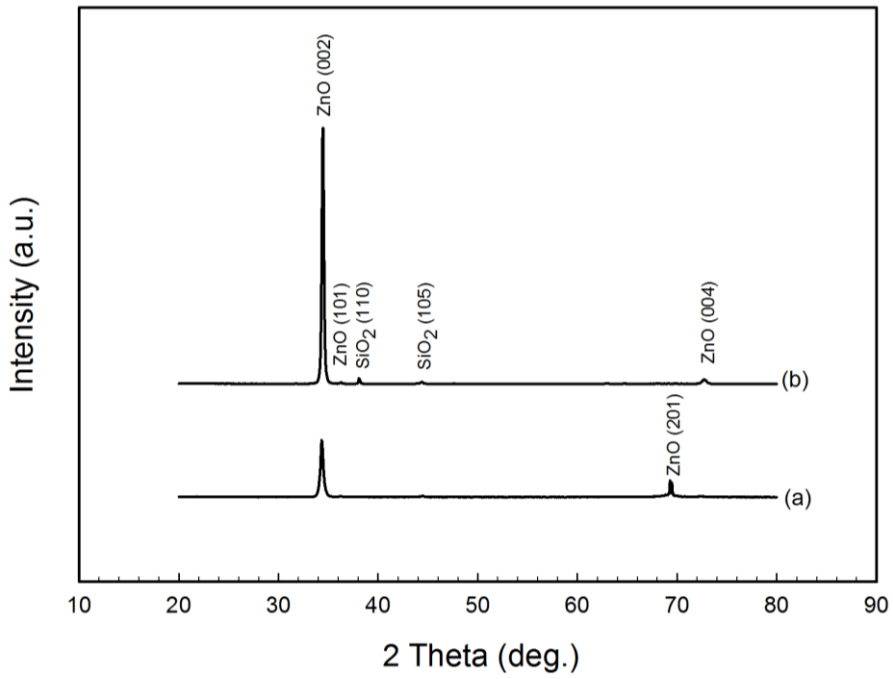

FIGURE 3. XRD patterns of the (a) as prepared and (b) heat treated ZnO films.

Both the Ag/ZnO/Ag (device A) and Al/ZnO/Ag (device B) MSM planar structure were used to analyse the UV photodetector performance, with dark and UV light illuminated current-voltage characteristic as shown in figure 4(a) and figure 4(b) respectively. The ZnO film for device B was first annealed at a temperature of 800 °C for 1 hr before the contacts were coated. The I-V characteristics for device A from -5 to 5 V exhibits back to back Schottky metal-semiconductor contacts with calculated Schottky barrier heights of 0.74 eV, which is 0.04 eV higher than published data reported by A. Y. Polyakov et al. (2003) and 0.10 eV lower than the estimated barrier height calculated by S. Liang et al. (2001). For device B the Schottky barrier heights is 0.76 eV which is 0.02 eV higher than device A. Both device structures showed considerable current-voltage effect upon illumination of UV light at 365 nm (figure 4(a) and (b)). For comparison the leakage current at 5 V bias are 18.6 mA and 0.6 µA for device A and B respectively. The photocurrents at 5 V bias are 24.2mA and 10.3 µA for device A and B respectively and are at a factor of 1.3 and 17.2 apart between them.

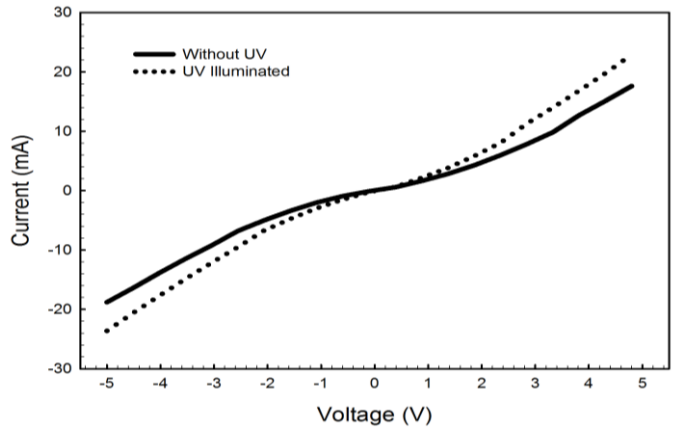

Figure 4(a): I-V characteristic of the Ag/ZnO/Ag MSM photodetector (device A) with and without UV illumination.

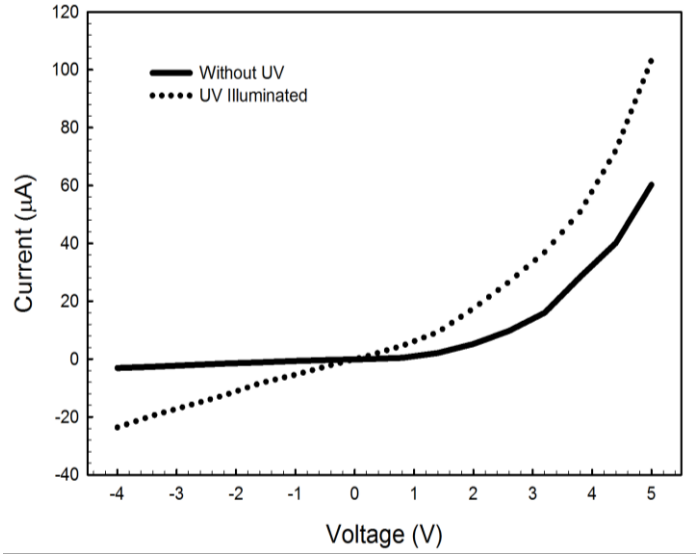

Figure 4(b): I-V characteristic of the Al/ZnO/Ag MSM Schottky photodetector with and without UV illumination.

The photoresponse of ZnO can be considered to be controlled by two main processes. The first is the rapid and reproducible solid-states process, whereby an optical photon of energy, larger than the band gap of the ZnO (hv>Eg = 3.37eV) incident on the depletion region, been absorbed and subsequently creating an electron-hole pair at the junction region. The second process is the adsorption and photodesorption of oxygen on the surface of ZnO film which is known as a slow process with a large response (Takahashi et al. 1994 and Li et al. 2005). This process can be described as follows: when the ZnO film is placed in the dark, oxygen molecules were adsorbed on the surface capturing an electron from the conduction band of ZnO.

$$O_2(g) + e^- \rightarrow O_2^-(ad) \quad (1)$$

This creates a depletion layer with high resistivity at the ZnO surface. Upon UV illumination photogenerated electron-hole pairs, will increase that led to the increase of probability of photogenerated hole, to be captured by the O_2^- species:

$$h^+ + O_2^-(ad) \rightarrow O_2(g) \qquad (2)$$

Photoresponse time of the various ZnO-based nanostructure film photodetectors to UV illumination in air, have been reported with large variations (rise times from 45.1ns to 5.9s; decay times from 1.678μs to 2710s) (Li et al. 2005; Zhen et al. 2008; Heesun et al. 2008; Bian et al. 2008; Liu et al. 2009 and Cheng et al. 2008) . The photoresponse of device A and B to UV illumination in air as a function of time at the bias of 4 V is shown in figure 5. The UV response rise time t_r (10% to 90%) for device A is approximately 125s and a decay time t_d of about 234s (90% to10%). The corresponding t_r for device B was found to be the same as for device A but the value of t_d was 212 s. The mechanism of the device UV response time can be explained by the two processes as stated earlier. We assume that in this work the contact metallization and the heat treatment might have affected the photoresponse time of the device.

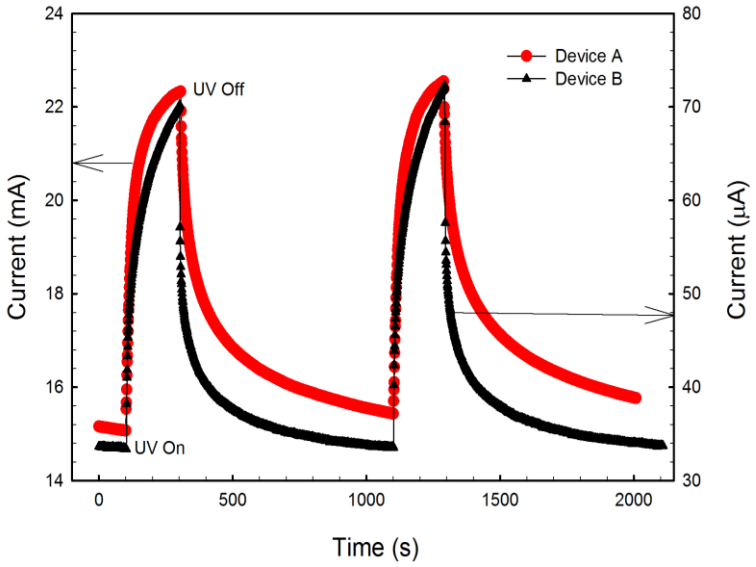

Figure 5: Photoresponse characteristic of the device A and device B photodetector at 4V

Figure 6 illustrates the PL spectra of the as prepared and annealed at 800 °C ZnO film. It is generally believed that the room temperature PL spectra for ZnO typically shows three major peaks which is orange emission at around 600 nm, a green emission peak around 520 nm and a UV peak emission peak at around 380 nm. The UV peak is attributed to band edge emission while the origin of the green and orange emissions that are caused by deep level emission is attributed to defect levels associated with oxygen vacancy and zinc interstitial (Studenikin *et al.* 1998 and Vanheusden *et al.* 1996). For the prepared ZnO sample, both the UV and green peaks are present at the wavelength of 378 nm and 512 nm. The presence of UV emission in ZnO could arise from band to band emission or excitonic recombination. The band to band energy is equal or higher than the band gap of ZnO, while the energy of excitonic recombination is lower than the band gap of ZnO. The prepared sample showed a UV peak at about 378 nm (~3.28 eV) which is distinctly lower than the band gap of ZnO at 3.37eV. In view of this we assumed that the UV emission from the prepared sample is caused by excitonic recombination. For the

annealed sample the ZnO film exhibits higher PL intensity at 480 to 550 nm wavelength regions. There is possibility, when ZnO films were annealed, more oxygen vacancies and zinc interstitial were created which could increased the deep level emission. The UV peak for the annealed sample shifted to a lower wavelength at 368 nm with lower intensity. This is lower than near band edge emission at 380 nm indicating that the emission might not have excitonic recombination but it could be caused by band to band transition which is about the same energy as that of the ZnO band gap at 3.37 eV.

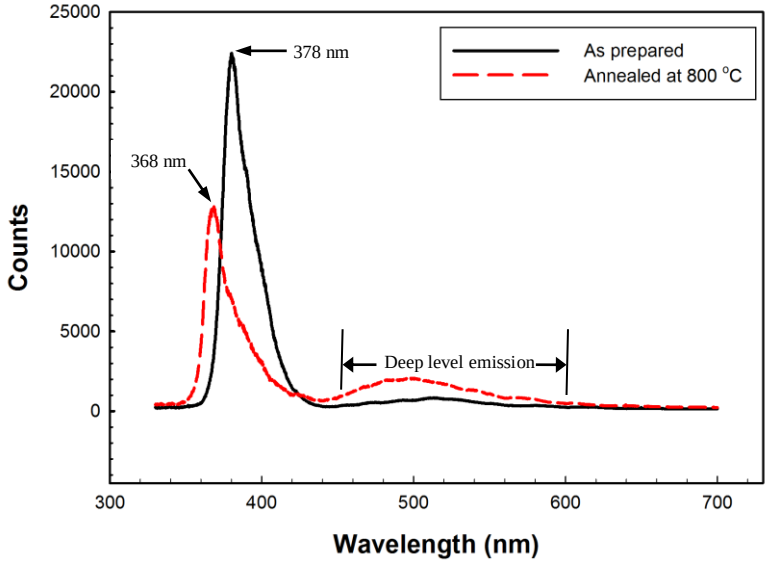

Figure 6: PL spectra for the as prepared and heat treated ZnO films.

4. Conclusion

ZnO films were successfully deposited on SiO_2/Si substrates by RF magnetron sputtering, MSM UV photodetector using Ag/ZnO/Ag configuration were fabricated from the as prepared film while the heat treated film was used to fabricate MSM Schottky barrier UV photodetector using Al/ZnO/Ag configuration. The crystalline and optical quality of the film has improved after the heat treatment. It was found that the Schottky barrier heights at the as prepared and heat treated Ag/ZnO interface was around 0.74 and 0.76 eV respectively. The leakage current was reduced from 18.6 mA to 0.6 µA at 5V after post deposition annealing when compared with that of as deposited ZnO. The Ag/ZnO/Ag showed a decay time of 212 s.

Acknowledgements

The main author of this paper is really grateful to UiTM Sabah for giving the opportunity to publish this work in the Journal of Borneo Akademika.

References

Ozgur U., Alivov Y.I., Liu C., Teke A., Reshchikov M.A., Do S., Doan S., Avrutin V., Cho S.J. and Morkoc H. 2005. *Journal of Applied Physics* 98: 041301.

Chunfeng W., Rongrong B., Kun Z., Taiping Z., Lin D and Caofeng P. 2015. *Nano Energy* 14: 364–371.

Vishnu A., Sushil Kumar P., Shruti V. and Shaibal M. 2016. *Journal of Luminescence* 180: 204–208.

Sandeep K.M., Shreesha B. and Dharmaprakash S.M. 2017. *Journal of Physics and Chemistry of Solids* 104: 36–44.

Jaber S., Ali F. and Tayebeh S. 2016. *Sensors and Actuators A* 247: 150–155.

Farhat O.F., Halim M.M., Ahmed N. M. and Qaeed M.A. 2016. *Superlattices and Microstructures* 100: 1120–1127.

Ke Z., Zhi Y., Minqiang W., Minghui C., Zhongwang S. and Jinyou S. 2017. *Sensors and Actuators A* 253: 173–180.
Shewale P.S., Lee N.K., Lee S.H., Kang K.Y. and Yu Y.S. 2015. *Journal of Alloys and Compounds* 624: 251–257.
Forat H. A., Z. Hassan. and Naser M. A. 2016. Optical Materials 60: 30–37.
Ghusoon M. A., James C. M., Ahmed K. K. and Cody T. 2014, *Sensors and Actuators A* 209: 16–23.
Shaivalini S. and Park S.H. 2015 *Superlattices and Microstructures* 86: 412–417.
YanT., Lua C.-Y.J., Schuberb R., Chang L., Schaadt D.M., Chou M.M.C., Ploog K.H. and ChiangC.-M. 2015 *Applied Surface Science* 351: 824–830.
Boukadhaba M.A., Fouzri A., Sallet V., Hassani S.S., Amiri G., Lusson A. and Oumezzine M. 2015, *Superlattices and Microstructures* 85: 820–834.
Liu H. F., Yang R. B., Guo S. F., Lee Coryl J.J. and Yakovlev N.L. 2017. *Journal of Alloys and Compounds* 703: 225–231.
Mariana S., Daniela G., Sergiu V. N., Adrian V. M. and Rodica P. 2017. *Applied Surface Science* 396: 1880–1889.
Lehraki N., Aida M.S., Abed S., Attaf N., Attaf A. and Poulain M. 2012. *Current Applied Physics* 12: 1283–1287.
André K., Sebastian E., Nicola S., Alessandra S., Jose F. B., Stephan G. and Frank A. M. 2017 *Applied Surface Science* 399: 282–287.
Girija K.G., Somasundaram K., Anita Topkar and Vatsa R.K. 2016 *Journal of Alloys and Compounds* 684: 15–20.
Kim S-H., Shim G-I. and Choi S-Y. 2017 *Journal of Alloys and Compounds* 698: 77–86.
Park Y.S., Litton C.W., Collins T.C. and Reynolds D.C. 1966. *Physical Review* 143:512.
Monroy E., Calle F., Pau J. L., Munoz E., Omnes F., Beaumont B. and Gibart P. 2001. *Journal of Crystal Growth* 230: 537.
Chai G. , Lupan O., Chow L. and Heinrich H. 2009. *Sensors and Actuators A* 150: 184–187.
Xu Q. A., Zhang J. W., Ju K. R., Yang X. D., Hou X. 2006. *Journal of Crsytal Growth* 289: 44–47.
Jun J. H., Seong H., Cho K., Moon B. M., Kim S. 2009. *Ceramic International* 35: 2797–2801.
Cheng J., Zhang Y., Guo R.. 2008. *Journal of Crystal Growth* 310: 57–61.
Liu J. M., Xia Y. B., Wang L. J., Shu Q. F., W. Shi M. 2007. *Journal Of Crystal Growth* 300: 353–357.
Bi Z., Zhang J, Bian X., Wang D., Zhang X., Zhang W. F., Hou X.. 2008. *Journal of Electric materials*, Vol 37, No. 5 760–763.
Liang S., Sheng H., Liu Y., Huo Z., Lu Y. and Shen H. 2001. *Journal Crystal Growth* 225: 110–113.
Yen T., Strome D., Kim S. J., DiNezza M., Cartwright A. N. and Anderson W. A. 2008. *Materials Research Society Symposium Proceedings* 1035 1035-L05–04.
Lin Y. Y., Chen C. W., Yen W. C., Su W. F., Ku C. H. and Wu J.J. 2008. *Applied Physics Letters* 92: 233301.
Lin T. K., Chang S. J., Su Y. K., Huang B. R., Fujita M. and Horikoshi Y. 2005. *Journal Of Crystal Growth* 281: 513–517.
Yadav H. K., Sreenivas K., and Gupta V. 2007. *Applied Physics Letters* 90: 17413.
Makino T., Segawa Y., Kawasaki M., Ohtomo A., Shiroki R, Tamura K., Yasuda T., Koinuma H. 2001. *Applied Physics Letters* 78: 1237.
Ohtomo A., Kawasaki M., Sakurai Y., Ohkubo I., Shiroki R., Yoshida Y., Yasuda Y., Segawa Y., Koinuma H. 1998. *Materials Science and Engineering* B56: 263–266.
Sun H. D., Makino T., Segawa Y., Kawasaki M., Ohtomo A., Tamura K., Koinuma H.. 2001. *Applied Physics Letters*. 78 (22): 3385–3387.
Hullavarad S. S., Hullavarad N. V., Pugel D. E., Dhar S., Venkatesan T. and Vispute R. D. 2008. *Optical Materials* 30: 993–1000
Tatsumi T., Fujita M., Kawamoto N., Sakajima M. and Horikoshi Y. 2004. *Japanese Journal of Applied Phys*ics Part 1 43 (5A): 2602–2606
Kim K. S., Kim H. W. and Lee C. M. 2003. *Materials Science and Engineering* B98: 135–139.
Yamada A., Sang B. and Konagai M. 1997. *Applied Surface Science* 112: 216.
Tang W. and Cameron D.C. 1994. *Thin Solid films* 238: 83–87.
Purica M., Budianu E., Rusu E., Daniela M. and Garnilla R.. 2002. *Thin Solid Films* 584: 403–404.
Wang Z. Y. and Hu L. Z.. 2009. *Vacuum* 83: 906–909.
Lee G.H., Yamamoto Y., Koufoji M. and . Ohtsu M. 2001. *Thin solid films* 386(1): 117–120.
Zhang J.P., He G., Zhu L.Q., Liu M., Pan S.S. and Zhang L.D.. 2007. *Applied Surface Science* 253: 9414–9421.
Takahashi Y., Kanamori M., Kondoh A., Minoura H. and Ohya Y. 1994. *Japanese Journal of Applied Phys*ics Part 1 33: 6611–6615.
Li Q. H., Gao T., Wang Y.G. and Wang T.H.. 2005. *Applied Physics Letters* 86 (12): 123117/1–123117/3.
Albertsson, J.; Abrahams, S. C.; Kvick, A. (1989). *Acta Crystallographica, Section B: Structural Science* B45 (1): 34–40.
You J.B., Zhang X.W., Fan Y.M., . Yin Z.G, Cai P.F. and Chen N.F.. 2009. *Applied Surface Science* 255: 5876–5880.
Polyakov A. Y., Smirnov N.B., Kozhukhova E.A. and Vdovin V. I.. 2003. *Applied Physics Letters* 83(8): 1575–1577.
Bi Z., Zhang J., Bian X., Wang D., Zhang X., Zhang W. F., Hou X.. 2008. *Journal of Electric materials*, Vol 37, No. 5.
Bae H., Im S., Song J.. 2008. *Japanese Journal of Applied physics* Vol 47: 5362–5364.
Bian X, Zhang J., Bi Z., Wang D., Zhang X., Hou X.. 2008. *Optical Engineering* 47 (6), 064001.

Liu C.Y., Zhang B.P., Lu Z.W., . Binh N.T, Wakatsuki K., Segawa Y., Mu R.. 2009. *The Journal of Materials Science: Materials in Electronics*. 20: 197–201.

S. A. Studenikin, N. Golego, and M. Cocivera.. 1998. *Journal of Applied physics* 84: 2287–2294.

Vanheusden K., Warren W.L., Seager C.H., Tallant D.R., Voight J.A.. 1996. *Journal of Applied physics* 79: 7983.